Kameda et al. Earth, Planets and Space (2021) 73:218
https://doi.org/10.1186/s40623-021-01462-9

Earth, Planets and Space

FULL PAPER

Open Access

Design of telescopic nadir imager for geomorphology (TENGOO) and observation of surface reflectance by optical chromatic imager (OROCHI) for the Martian Moons Exploration (MMX)

Shingo Kameda[1,2*], Masanobu Ozaki[2], Keigo Enya[2], Ryota Fuse[3], Toru Kouyama[4], Naoya Sakatani[1], Hidehiko Suzuki[5], Naoya Osada[1], Hiroki Kato[1], Hideaki Miyamoto[6], Atsushi Yamazaki[2], Tomoki Nakamura[7], Takaya Okamoto[2], Takahiro Ishimaru[2], Peng Hong[8], Ko Ishibashi[8], Takeshi Takashima[2], Ryoya Ishigami[9], Cheng-Ling Kuo[10], Shinsuke Abe[3], Yuya Goda[11], Hajime Murao[11], Saori Fujishima[11], Tsubasa Aoyama[11], Keiji Hagiwara[11], Satoko Mizumoto[11], Noriko Tanaka[11], Kousuke Murakami[12], Miho Matsumoto[12], Kenji Tanaka[12] and Hironobu Sakuta[12]

Abstract

The JAXA's Martian Moons Exploration (MMX) mission is planned to reveal the origin of Phobos and Deimos. It will remotely observe both moons and return a sample from Phobos. The nominal instruments include the TElescopic Nadir imager for GeOmOrphology (TENGOO) and Optical RadiOmeter composed of CHromatic Imagers (OROCHI). The scientific objective of TENGOO is to obtain the geomorphological features of Phobos and Deimos. The spatial resolution of TENGOO is 0.3 m at an altitude of 25 km in the quasi-satellite orbit. The scientific objective of OROCHI is to obtain material distribution using spectral mapping. OROCHI possesses seven wide-angle bandpass imagers without a filter wheel and one monochromatic imager dedicated to the observation during the landing phase. Using these two instruments, we plan to select landing sites and obtain information that supports the analysis of return samples.

Keywords: MMX, TENGOO, OROCHI, Imager, Phobos, Deimos, Mars

*Correspondence: kameda@rikkyo.ac.jp
[1] Rikkyo University, Tokyo, Japan
Full list of author information is available at the end of the article

Graphical Abstract

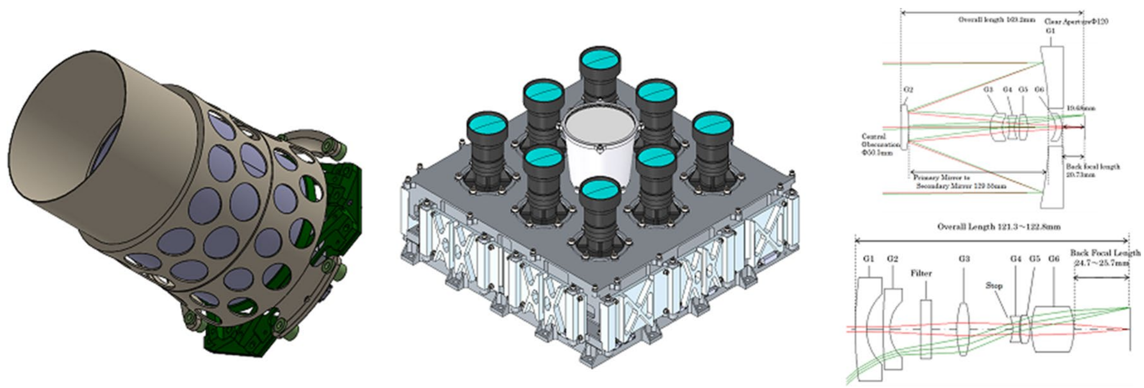

Introduction

Japan Aerospace Exploration Agency (JAXA)'s Martian Moons Exploration (MMX) is planned to be a sample return mission from Phobos, one of the satellites of Mars. The instrument complement includes the telescopic nadir imager for geomorphology (TENGOO), optical radiometer composed of chromatic imagers (OROCHI), MMX infrared spectrometer (MIRS) (Barucci et al. 2021), Mars-moon exploration with gamma rays and neutrons (MEGANE) (Lawrence et al. 2019), mass spectrum analyzer (MSA) (Yokota et al. 2021), circum-Martian dust monitor (CMDM) (Krüger et al. 2021), light detection and ranging (LIDAR) (Senshu et al. 2021) and Rover (Michel et al. 2021). One of the scientific objectives of MMX is to determine the origin of the two Martian moons (Kuramoto et al. 2021). Phobos and Deimos seem to be asteroids captured by Mars' gravity, according to spectroscopic observation of the surface reflectance. Conversely, they may have been formed by a large impact of a body with Mars and subsequent accretion, according to their circular and low-inclination orbit. Because the composition should be highly dependent on their origin, elemental analysis will clarify the origin of the moons.

We should select the landing site where the flatness is lower than 0.3 m in the diameter range of 5 m for safe landing of the MMX spacecraft. TENGOO is a telescopic camera, which is to acquire highest-resolution images from the quasi-satellite orbit for landing site selection. In the landing phase, the MMX mission will acquire more than 10 g of regolith on the surface of Phobos (Usui et al. 2020; Fujiya et al. 2021). It will include a coring unit with a core diameter of 25 mm. Assuming that the sample is representative of Phobos, we will be able to clarify the origin of the moons.

To test this assumption, we will identify suitable landing sites and characterize the uniformity or nonuniformity of the distribution of the surface material. OROCHI is

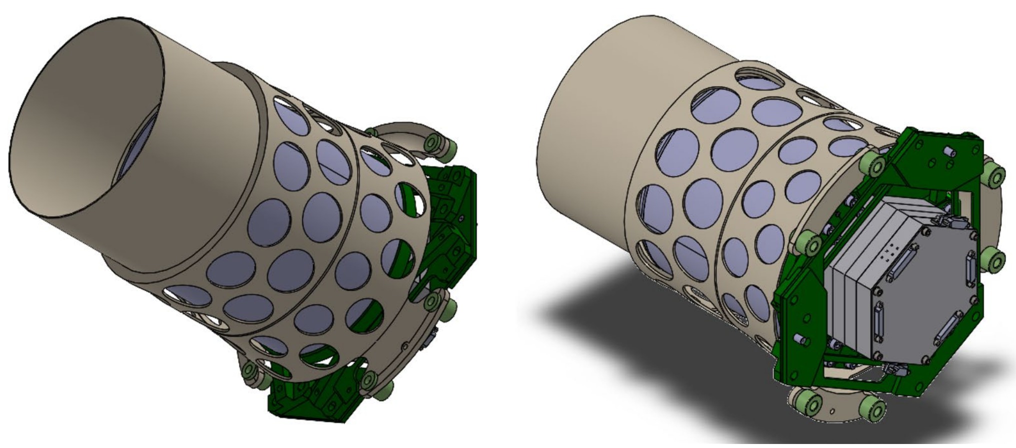

Fig. 1 External views of TENGOO-S

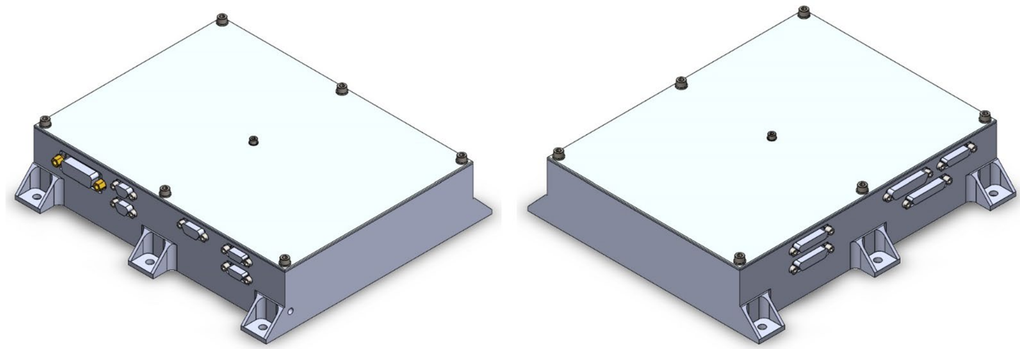

Fig. 2 External views of TENGOO-E

a wide-angle multi-band imager, which enables the acquisition of spectral images of the moons with high spatial resolutions of less than 25 mm. We can obtain global images from the quasi-satellite orbit and highest-resolution images during the landing operation. We also plan to observe the Mars climate from the orbit when we do not observe Phobos or Deimos (Ogohara et al. 2021). In this paper, we describe the requirements for TENGOO and OROCHI and present our preliminary design.

Performance requirements

One of the mission objectives of MMX is to spectroscopically reveal the surface-layer distribution of the materials that constitute Phobos with the spatial resolution required for the scientific evaluation of sampling points and geological structures, thereby constraining the Phobos' origin (Kuramoto et al. 2021). To achieve this objective, the MMX instrument complement will obtain, spectroscopically, the distributions of hydrous minerals and overlay them over a global map of the topography at horizontal spatial resolutions of below 20 m because there is a statistically significant number (10 or more) of boulders of 20 m or more (Thomas et al. 2000). We will perform global imaging operation when the MMX spacecraft will be in the quasi-satellite orbit (QSO) around Phobos; the typical altitude is ~ 20 km in the QSO-low (Nakamura et al. 2019). For Deimos flyby observation, the required spatial resolution is 100 m and the flyby distance will be 100 km (Nakamura et al. 2019). Thus, an angular resolution below 1 mrad is required. Therefore, we set the OROCHI's instantaneous field of view (iFoV) to 0.5 mrad/pix. We selected seven bands for spectroscopy. The center wavelengths are 390, 480, 550, 650, 730, 860, and 950 nm, while the bandwidths are 50, 30, 30, 40, 40, 40, and 60 nm, respectively. The wavelengths of 390, 480, 550, 860, and 950 nm are the same as those of the ul-, b-, v-, x-, and p-bands of the optical navigation camera telescope (ONC-T) onboard the Hayabusa2 spacecraft (Kameda et al. 2017), which has seven band-pass filters. We selected the wavelengths of 650 and 730 nm to characterize the absorption around 650 nm,

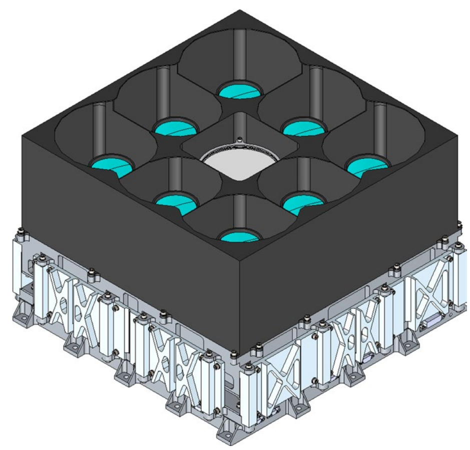

Fig. 3 External view of OROCHI

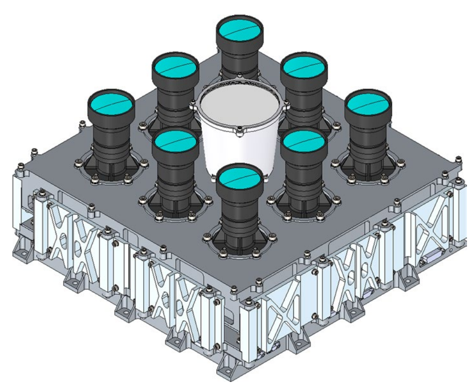

Fig. 4 External view of OROCHI without hood

specific to the red unit of Phobos (Kuramoto et al. 2021; Fraeman et al. 2014). The requirement for image quality was the modulation transfer functions (MTFs) of optics at Nyquist frequencies of above 0.3 for 480–860 nm and above 0.2 for 390 and 950 nm. The signal-to-noise ratio (SNR) should be higher than 100 to detect the absorption around 650 nm, the depth of which is approximately 3–4%.

We should obtain material distributions spectroscopically at a radius of 50 m or larger around the sampling site (at spatial resolutions of 1 m or better) (Kuramoto et al. 2021). In the current operation plan, the MMX spacecraft will be right above the landing site at altitudes < 1 km in the descent phase (Nakamura et al. 2019). Thus, the required angular resolution is the same as that above.

One or more images near the sampling point should be taken at the landing operation. The average distance between OROCHI and the surface of Phobos is designed to be ~ 0.8 m. The field of view (FoV) should be above 1 rad to obtain an image of the sampling point. The spatial resolution should be below 5 mm for multi-band images, which corresponds to ~ 1/5 of the diameter of the sample core. The spatial resolution of monochromatic images should be below 1 mm.

Images with resolutions below 0.3 m are required for landing site selection. To satisfy this requirement, we set the performance requirement for TENGOO as follows. The iFoV should be below 6 μrad/pix, while the MTF of optics at Nyquist frequency should be above 0.2, which is the lower limit to identify undulations at the size of above 2 pixels. The size of the lowest QSO is 20 km × 27 km in the current plan (Nakamura et al. 2019); thus, the altitudes of the spacecraft are approximately 10–17 km. If the iFoV is 6 μrad/pix, 2 pixels correspond to ~ 0.2 m at an altitude of 17 km. To find a flat area for landing, we plan to obtain images of the shadows of the large boulders with high phase angles more than 60 degrees. Then, the mission could select the landing site from the QSO.

Instrument design

Design overview of TENGOO

TENGOO possesses a camera and interface component, TENGOO-S, which is composed of optics, image sensor, analog front-end electronics (AFE), and analog-to-digital conversion (ADC) function, and TENGOO-E, which has a field-programmable gate array (FPGA), secondary power supply, and communication functions with the spacecraft system. TENGOO-S operates at distances of less than 2 m from TENGOO-E. Figures 1 and

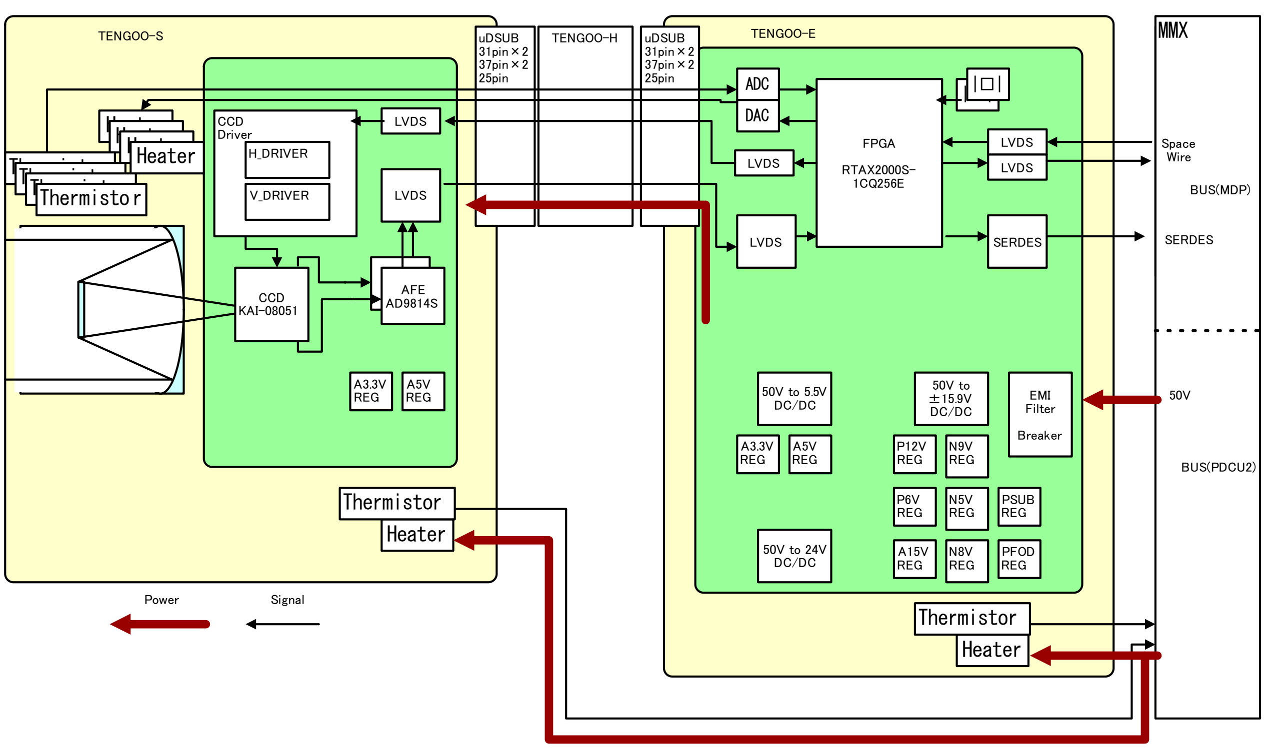

Fig. 5 TENGOO block diagram

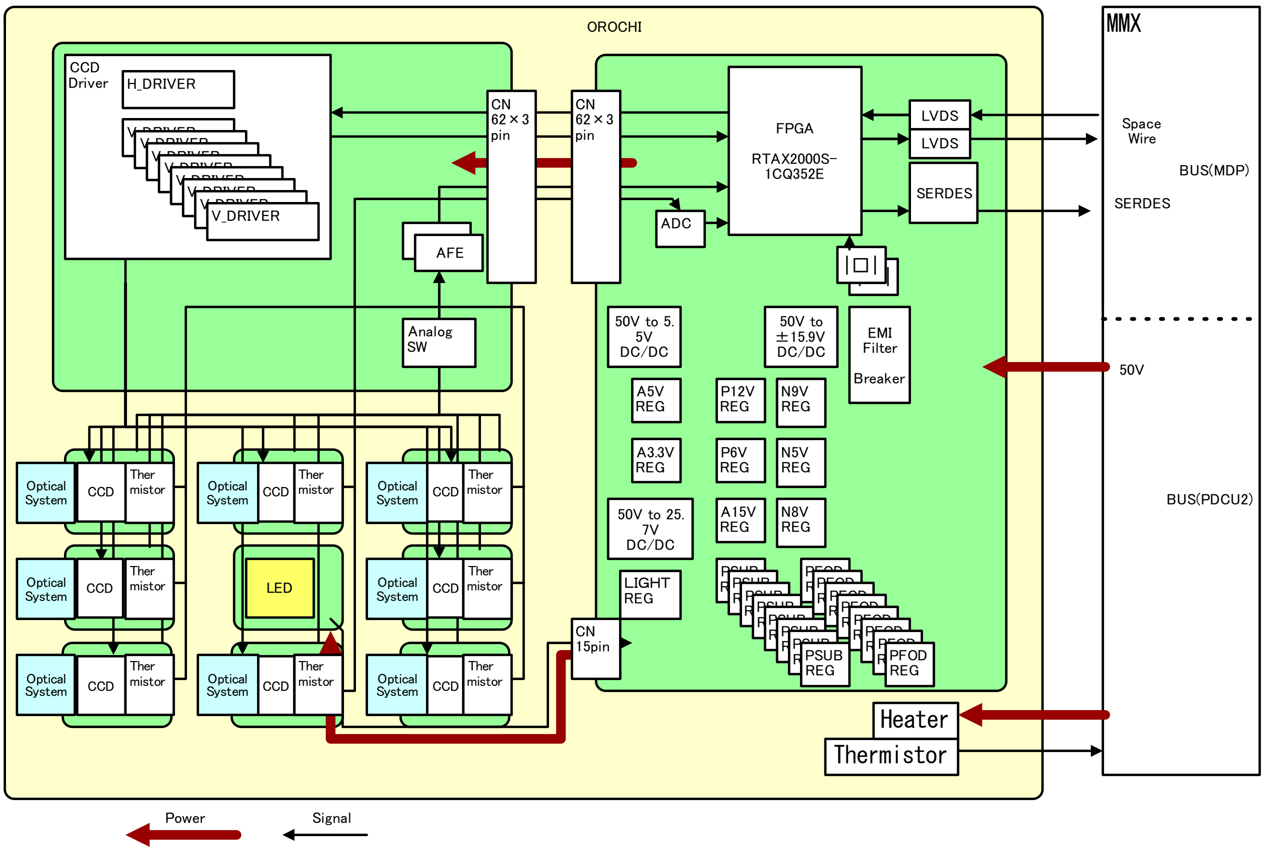

Fig. 6 OROCHI block diagram

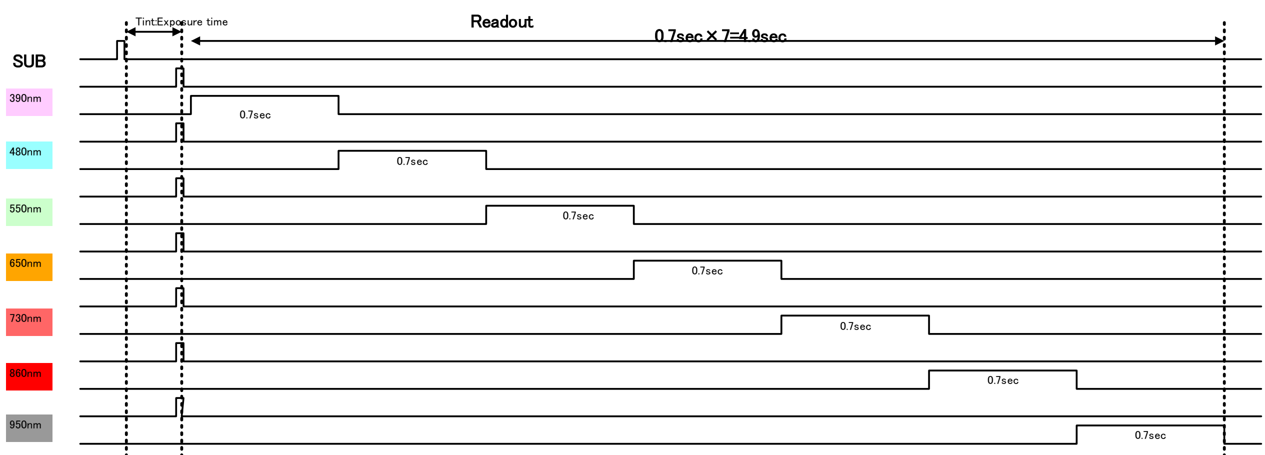

Fig. 7 OROCHI readout timing diagram for simultaneous seven-band imaging

2 show external views of TENGOO-S and TENGOO-E, respectively.

TENGOO-S has a catadioptric Cassegrain telescope. Its focal length is 947.8 mm, and the effective F-number is 8.9. The detector is an interline charge-coupled device

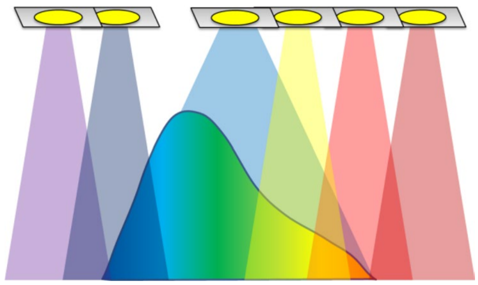

Fig. 8 Conceptual diagram of the system of a white LED and five monochromatic LEDs (390, 480, 730, 860, and 950 nm)

(CCD), (KAI-08051). The pixel pitch of the CCD is 5.5 μm, while the number of pixels is 3296 × 2472. Thus, the iFoV is 5.9 μrad, while the diagonal FoV is 1.34°. The optical system is panchromatic and consists of a primary mirror, secondary mirror, and corrective lens system consisting of four lenses.

The masses of TENGOO-S and -E are 4.8 and 1.2 kg, respectively. The dimensions of TENGOO-S and E are ϕ301.2 mm × 352.5 mm and 201.2 mm × 181.2 mm × 49.5 mm, respectively. The storage temperature is −30 to +60 °C. The temperature of the telescope should be maintained at +20 ± 5 °C during observation.

Design overview of OROCHI

OROCHI has a camera part and interface part in one housing. For multi-band observations, OROCHI has seven bandpass filters, seven optical paths, seven CCD image sensors and no filter wheel. The center wavelengths are 390, 480, 550, 650, 730, 860, and 950 nm, and the bandwidths are 50, 30, 30, 40, 40, 40, and 60 nm, respectively. Although Hayabusa2/ONC-T had a filter wheel, we did not use one on OROCHI. The ONC-T's filter wheel possesses a limited number of rotations. If it stops in the middle of changing the filter, no further observations can be carried out. In addition, when the ground speed is high, particularly during the descent phase, the FoV moves while the filter is being changed. OROCHI fields seven independent bandpass imagers to avoid these problems. In addition, OROCHI includes a monochromatic camera (550 nm) dedicated to the observation during the landing phase. The spatial resolutions of the seven bandpass imagers are below 5 mm but above

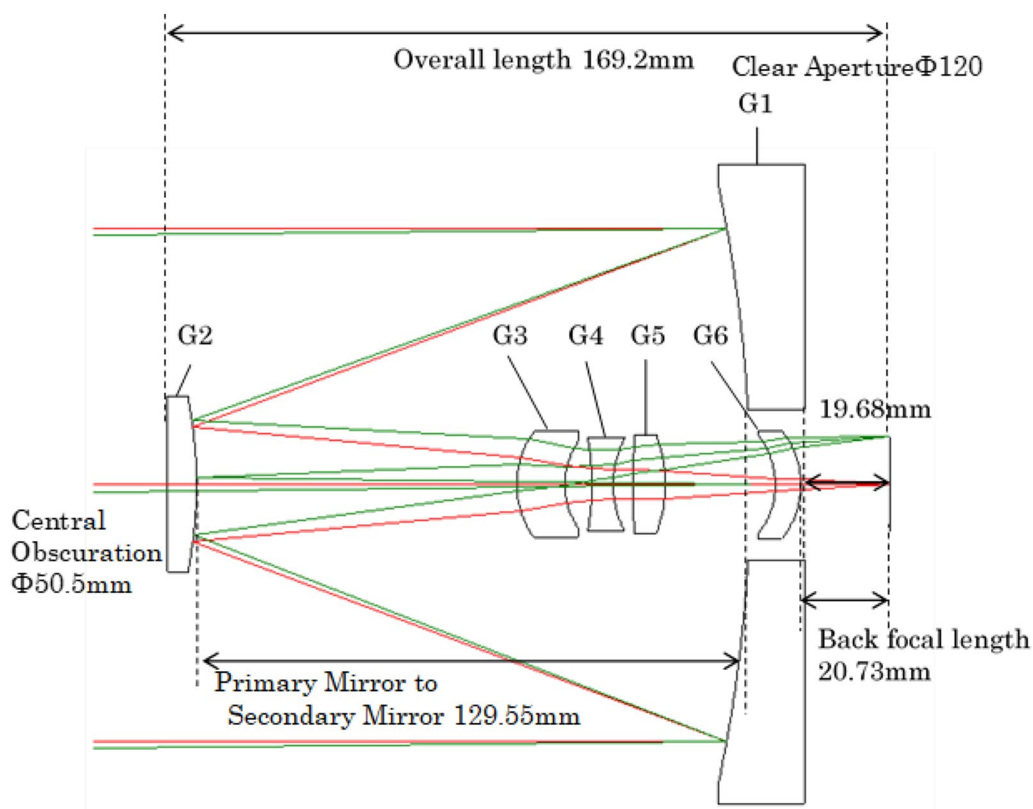

Fig. 9 TENGOO optical design schematic

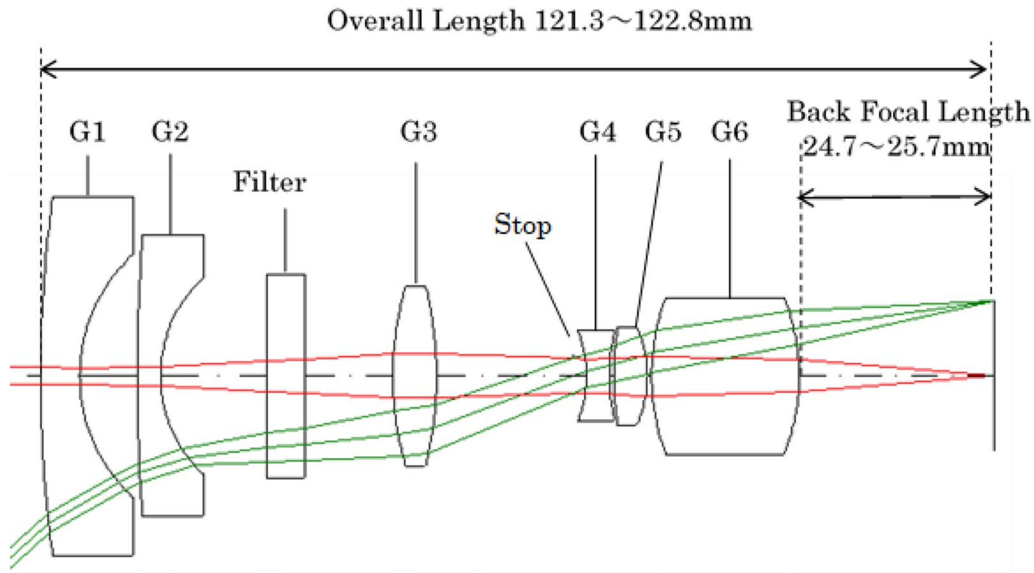

Fig. 10 OROCHI optical design schematic

1 mm because of the out-of-focus at a short distance (~0.8 m). The focus of the monochromatic camera is adjusted for a distance of 0.8 m and its spatial resolution is ~0.7 mm. Thus, OROCHI has eight cameras in total. During the landing phase, the sample collection location may be in the shadow of the spacecraft. To prepare for such cases, OROCHI has a light emitting diode (LED) module that can illuminate the dark region. Figures 3 and 4 show external views of OROCHI with and without hood, respectively.

The OROCHI's eight optical pathway are almost identical; however, some gaps between lenses, aperture stop, etc., are optimized for each band. Its focal length is 13.23–13.57 mm, and effective F-number is 5.8–6.4. The detectors are interline CCDs (KAI-08051). The pixel pitch of the CCD is 5.5 μm and the number of pixels is 3296 × 2472. Thus, the iFoV is 0.44–0.46 mrad/pix, while the diagonal FoV is 83–85.5°.

The mass of OROCHI is 12.13 kg. Its dimensions are 243 mm × 368 mm × 368 mm. The storage temperature is −30 to +60 °C and the operation temperature is −20 to +55 °C.

Detectors and electronics

TENGOO and OROCHI use the same CCD, the ONSemi KAI-08051. It is an interline CCD. Its total number of pixels is 3364 × 2520, which includes dark reference pixels, and the number of active pixels is 3296 × 2472. We performed a comparative study between KAI-08051 and KAI-08052. KAI-08052 is a newer type of detector, which is approximately twice as sensitive in the near-infrared range, but has approximately three times higher dark current. During the landing phase, we expect the temperature of the instrument to increase, which increases the dark current, which is disadvantageous when LEDs are used to illuminate areas in the shadow of the spacecraft and acquire images with long exposure times. In order to ensure low development costs, we chose KAI-08051 for all CCD image sensors used in TENGOO and OROCHI.

Figures 5 and 6 show block diagrams of TENGOO and OROCHI, respectively. TENGOO has two AFEs for readout and uses two CCD output ports to increase the speed of the readout. The highest frame rate is 1.15 frame/s. TENGOO-E receives commands and sends out telemetry through SpaceWire (SpW). We use the high-speed serial interface Serializer Deserializer (SERDES) for the transmission of the imaging data. Both SpW and SERDES are redundant in systems A and B. The power consumption of TENGOO is approximately 7 W in standby and approximately 15 W in imaging and readout.

OROCHI has almost the same electronics as TENGOO. It has only two AFEs for readout. Eight cameras are connected to the switch in parallel; therefore, it is not possible to read from more than two cameras simultaneously. For simultaneous imaging in multiple bands, OROCHI reads out up to seven wavelengths in sequence. Figure 7 shows the CCD readout timing diagram for simultaneous imaging at seven wavelengths with OROCHI. As an illumination method for the landing phase, we use a combination of a white LED and multiple monochromatic LEDs. Figure 8 shows a conceptual diagram of the system of a white LED and five monochromatic LEDs (390, 480, 730, 860, and 950 nm). Only the white LED is used at 550 and 650 nm because of its high intensity at these wavelengths. This unit can illuminate the area within a circle with a radius of 0.25 m and the brightness of the illuminated area becomes brighter than 1/100th of that of the sunlit surface. The power consumption of OROCHI is approximately 7 W in standby and 18 W in imaging and readout. The power consumption of the illumination unit is approximately 30 W in total.

Optical design

The optical system of TENGOO is catadioptric and consists of two mirrors (primary and secondary) and correction lens consisting of four lenses. An optical design schematic of TENGOO is shown in Fig. 9. This catadioptric Cassegrain system consists of rotationally symmetric aspheric primary and secondary mirrors and four spherical corrective lenses. The effective diameter of the primary mirror is 120 mm, and the diameter of the shielded part is 50.5 mm. In the order in which the incident light is reflected or transmitted, there is a primary mirror (G1), secondary mirror (G2), and corrective lenses (G3–6), leading to the sensor. The glass material is all fused silica for radiation tolerance. The length from the surface closest to the object to the sensor is 169.2 mm and the outer diameter of the primary mirror is 149.6 mm.

The OROCHI optical system is a retrofocus type and consists of eight optical systems, seven for each observation wavelength and one for monochromatic imaging. An optical design schematic of the optics of OROCHI for a center wavelength of 550 nm is shown in Fig. 10. The eight optical systems differ in the radius of curvature of the surface on the sensor side of G3, gap between G2 and G3, aperture diameter, and filter for each wavelength range and for monochromatic imaging. The spacing between G2 and G3 is adjusted for each wavelength range to reduce the effects of manufacturing errors. The differences in the optical systems for each wavelength and for monochromatic imaging are minor; structurally, they are almost identical. The outer diameter of G1 is 46 mm. At the center wavelength of 550 nm, the length from the first surface of the optical system to the sensor is 121.9 mm.

As shown in Fig. 10, the filter is placed between G2 and G3, located far away from the sensor to reduce stray light due to reflection between the filter and sensor and minimize the difference in the angle of incidence across the FoV to reduce the effect of the dependence of the filter on the angle of incidence. We made the back focus (distance from G6 to the sensor) long to reduce stray light due to reflection between G6 and the sensor. It is set to 24.9 mm at the center wavelength of 550 nm.

Radiometric performance

The SNR required for TENGOO for topographic observation is > 30. We calculated the surface brightness of Phobos under the following conditions:

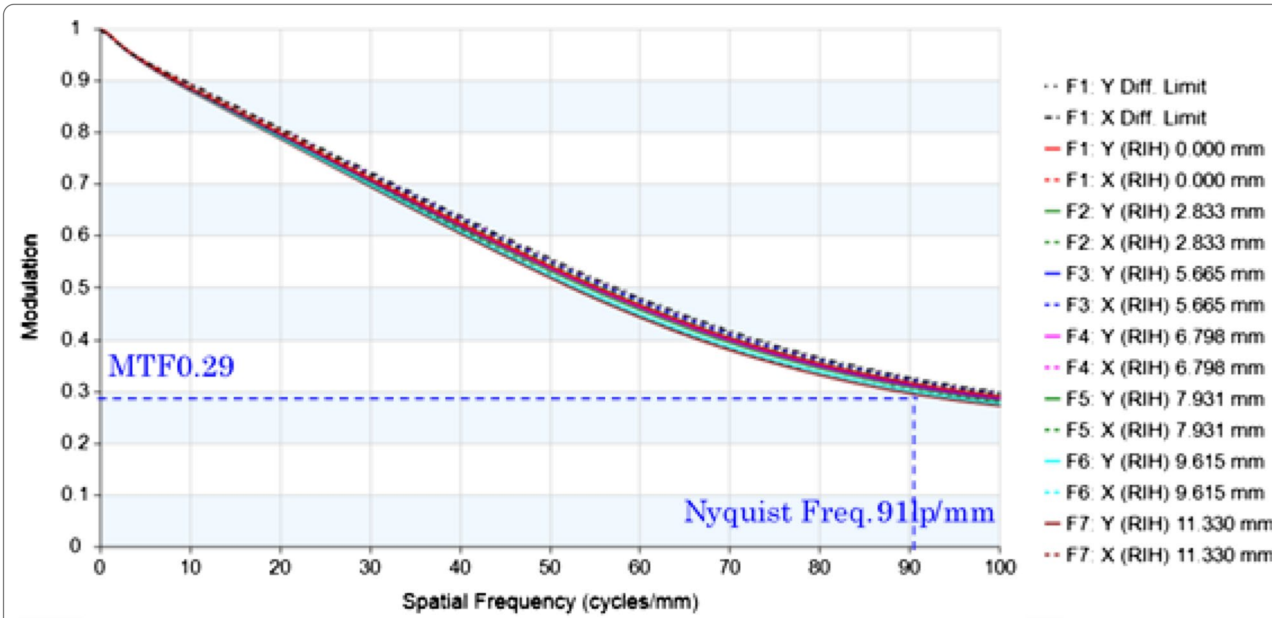

Fig. 11 TENGOO optics MTF

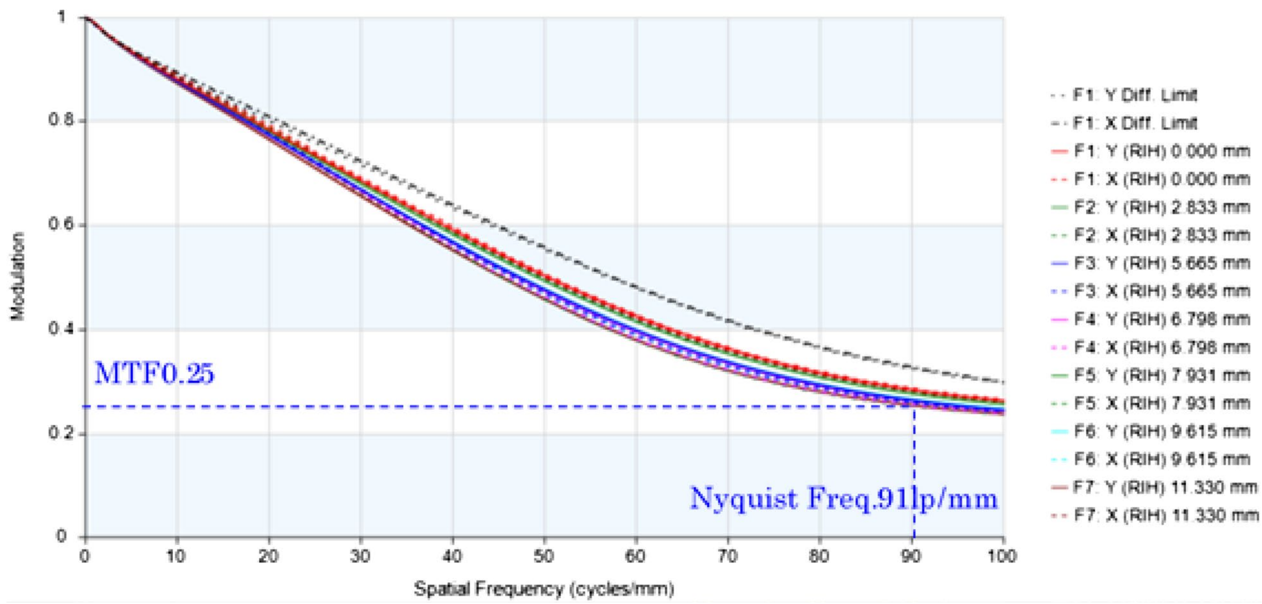

Fig. 12 TENGOO optics MTF at − 5 °C relative to the nominal temperature

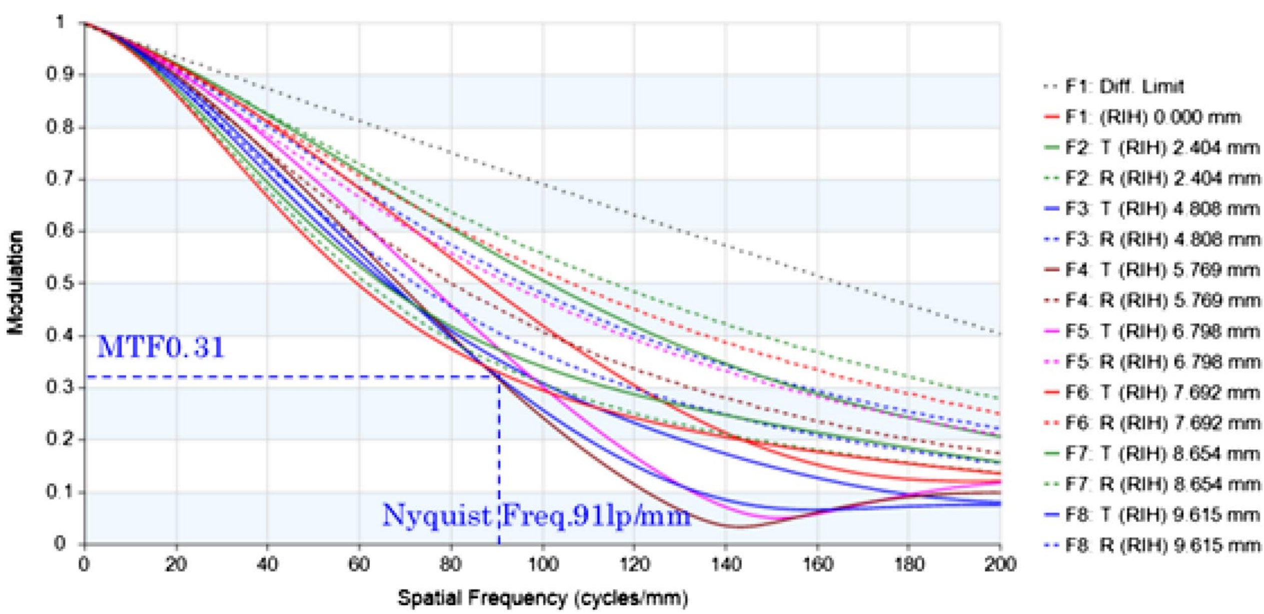

Fig. 13 MTF vs spatial freq. design nominal at objective distance 20 km (central wavelength 390 nm, bandwidth 50 nm)

1. The distance of Mars from the Sun is 1.666AU (aphelion).
2. The incidence angle of sunlight is 30° and the emission angle is 0°.
3. Phobos has a Lambertian surface with a reflectance of 7%.

We calculated the signal from the surface brightness, the optical system transmittance, and the quantum efficiency of the CCD. We calculated the random noise as the root sum square of statistical noise, readout noise, and dark current noise. We will correct the dark current by subtracting the dark image from the observed image in operation. When Phobos and Mars are out of the FoV,

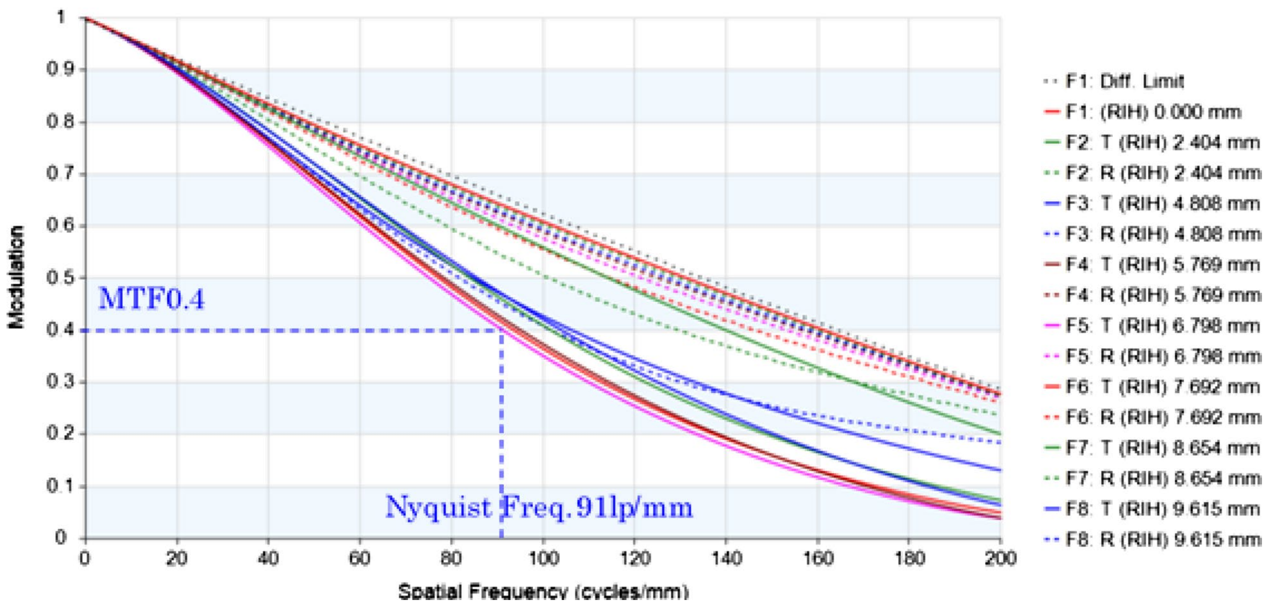

Fig. 14 MTF vs spatial freq. design nominal at objective distance 20 km (central wavelength 480 nm, bandwidth 30 nm)

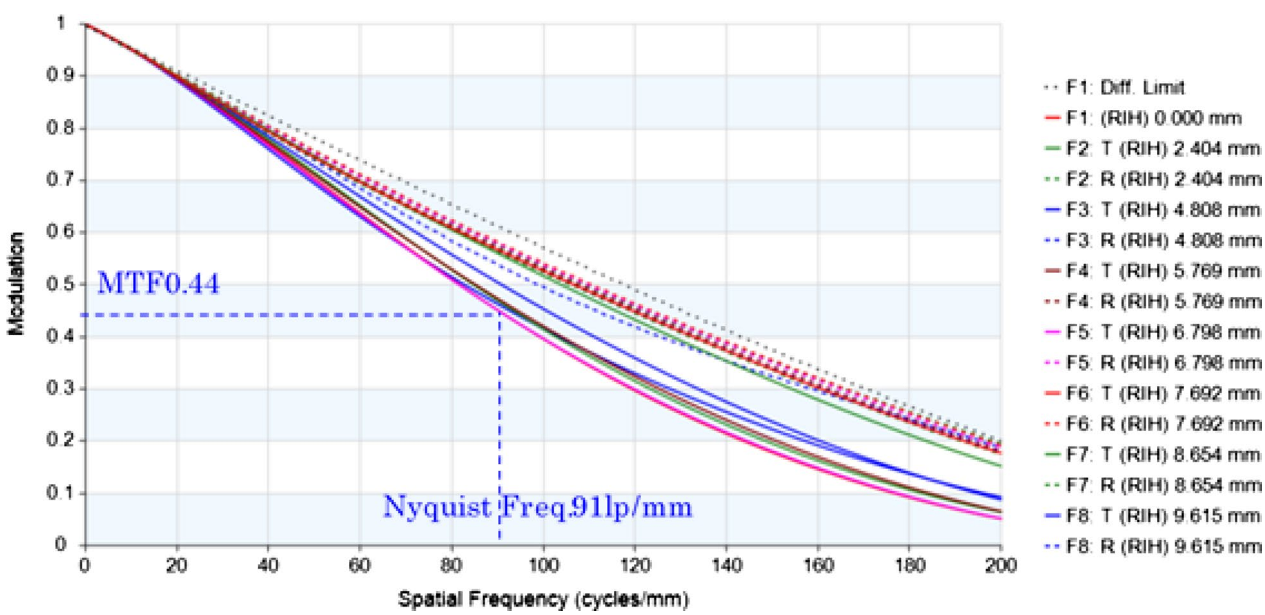

Fig. 15 MTF vs spatial freq. design nominal at objective distance 20 km (central wavelength 550 nm, bandwidth 30 nm)

we will acquire multiple dark images in different viewing directions, and use the portion without stars. Here, we assumed the CCD temperature is + 30 °C for the highest dark current case. As a result, the exposure time should be longer than 1.2 ms for SNR > 30. The ground speed at QSO is approximately 3 m/s, thus the shift of FoV in this exposure time (36 mm) is nearly an order of magnitude smaller than the required resolution (0.3 m). The attitude stability of the spacecraft is < 3 μrad (3 σ) for 10 ms, which corresponds to 1/2 pixel, thus the blurring of the image during this exposure time is also sufficiently smaller than the required resolution.

The SNR required for OROCHI for spectroscopic observation is > 100. The F-numbers are 6.4 for

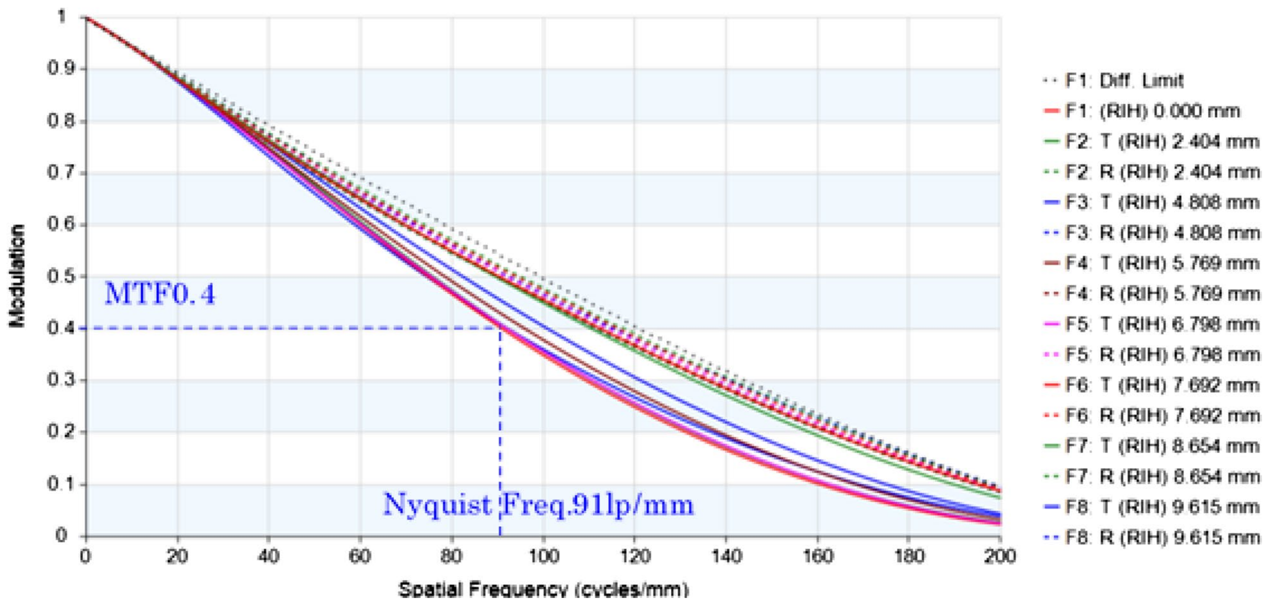

Fig. 16 MTF vs spatial freq. design nominal at objective distance 20 km (central wavelength 650 nm, bandwidth 40 nm)

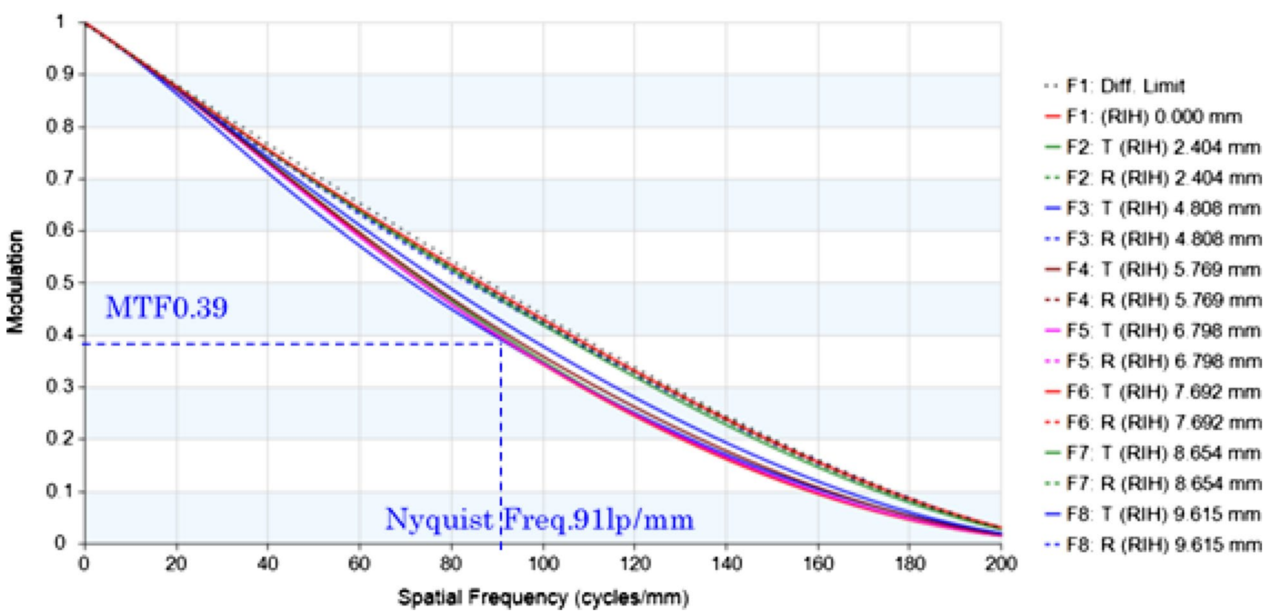

Fig. 17 MTF vs spatial freq. design nominal at objective distance 20 km (central wavelength 730 nm, bandwidth 40 nm)

390–730 nm, 6.2 for 860 nm, and 5.8 for 950 nm. As a result, the exposure times for SNR of 120 are 0.099 s for 390 nm, 0.071 s for 480 nm, 0.074 s for 550 nm, 0.086 s for 650 nm, 0.14 s for 730 nm, 0.49 s for 860 nm, and 0.84 s for 950 nm. The shift of FoV in an exposure time of 1 s is ~ 3 m, which satisfies the requirement with significant margin for a resolution of 20 m required for QSO observation. The attitude stability of the spacecraft is < 0.17 mrad (3 σ) for 1 s, which corresponds to 0.4 pixels, thus the blurring of the image during the shorter exposure time is also sufficiently smaller than the required resolution.

We need longer exposure time when we obtain the image of the surface in the shadow of spacecraft using

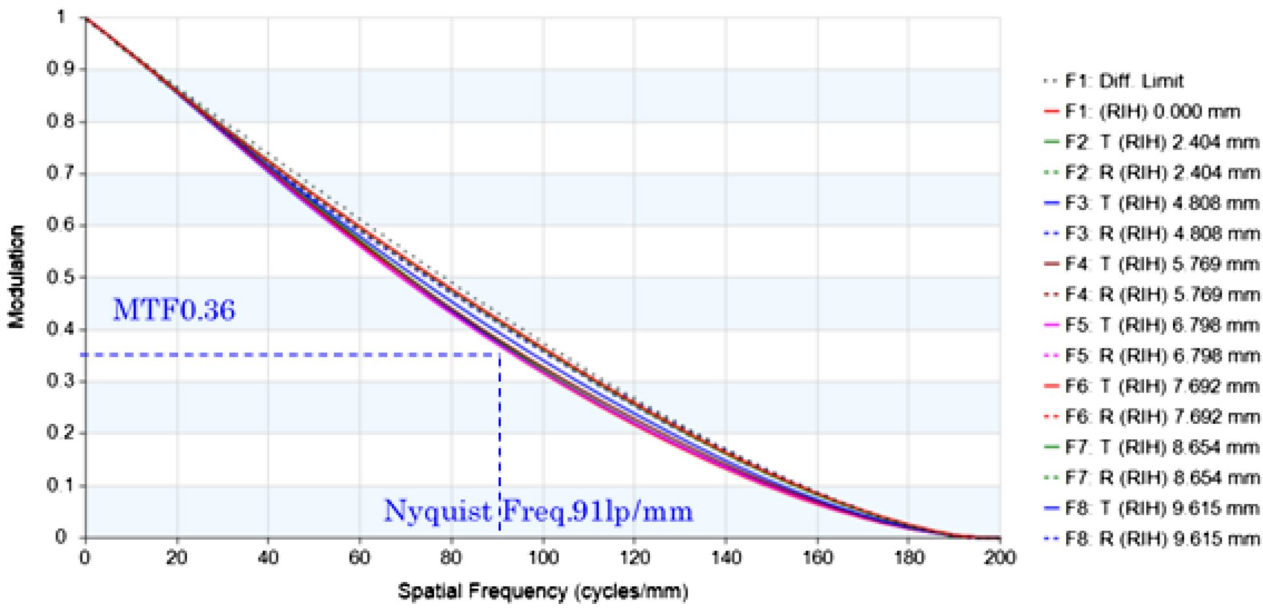

Fig. 18 MTF vs spatial freq. design nominal at objective distance 20 km (central wavelength 860 nm, bandwidth 40 nm)

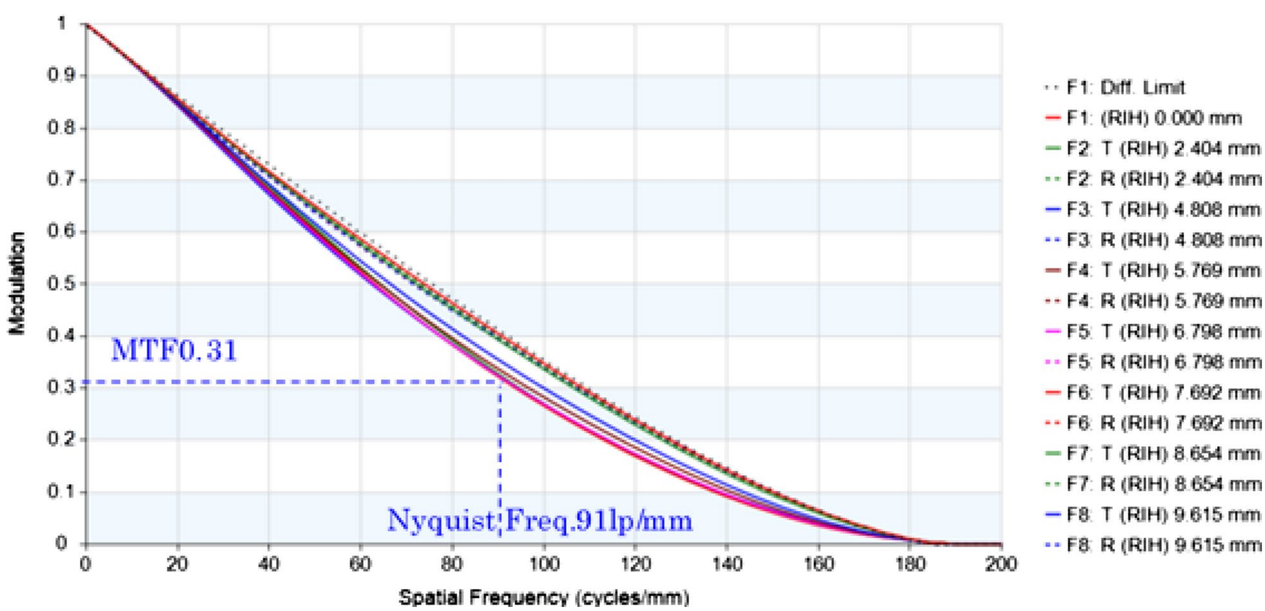

Fig. 19 MTF vs spatial freq. design nominal at objective distance 20 km (central wavelength 950 nm, bandwidth 60 nm)

the LED illumination because the surface brightness is 1/100th of that of the sunlit surface. To achieve SNR > 100, we have to use 2 × 2 binning mode and the required exposure times are 4.84 s, 3.56 s, 3.64 s, 4.39 s, 7.14 s, 26.7 s, and 52.4 s, respectively. We will perform the long exposures while the spacecraft is stationary on Phobos surface; thus motion blur will be negligible. In addition, we have to take multiple images with shorter exposure time for 860 nm and 950 nm because the number of integrated electrons exceed the full well capacity of CCD. The stray light from the sunlit surface will be less than the signal from the LED-illuminated area and negligible after subtracting the image without the LED illumination.

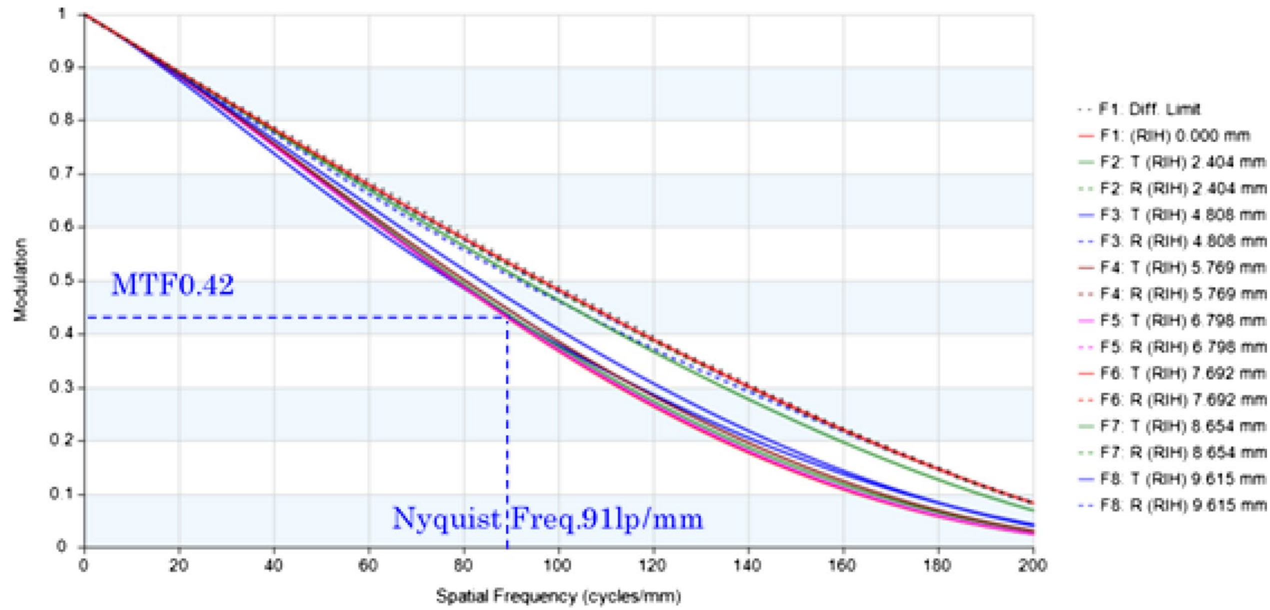

Fig. 20 MTF vs spatial freq. design nominal at objective distance 0.8 m (central wavelength 550 nm, bandwidth 30 nm)

Optical resolution

The MTFs of TENGOO cover the spectral range of 350–950 nm. Here we have considered the spectrum of incident flux, quantum efficiency of the detector, and optics transmittance. The result is shown in Fig. 11. The MTF at Nyquist frequency (91 lp/mm) is more than 0.29 in design. Although invar, a material with low thermal expansion, is used in the support structure of the telescope, the temperature of the telescope needs to be controlled within a range of ± 5 °C to keep the spacing between the primary and secondary mirrors. Figure 12 shows the MTF at Nyquist frequency is 0.25 at -5 °C relative to the nominal temperature and the guaranteed smallest value of MTF is 0.2. Note that the change in MTF when the pressure changes from ambient to vacuum is negligible because the refractive power is mainly carried by the mirror.

We computed the MTF of OROCHI was calculated by assigning the same weight to the three wavelengths of the central, longest, and shortest wavelengths for each band (e.g., for a central wavelength of 390 nm and a bandwidth of 50 nm, we assigned the same weight to the three wavelengths of 415 nm, 390 nm, and 365 nm). The calculated MTFs for each band are shown in Figs. 13, 14, 15, 16, 17, 18 and 19. The nominal values of MTFs at the Nyquist frequency (91 lp/mm) are 0.31–0.44 at a distance of 20 km over the entire FoV. As shown in Fig. 20, the MTF at the Nyquist frequency is 0.31 over the entire FoV for monochromatic imaging during the landing phase at a distance of 0.8 m with a center wavelength of 550 nm and a bandwidth of 30 nm.

Summary

The scientific objectives of TENGOO and OROCHI are to use spectral mapping and imaging to obtain the geomorphological features and material distribution of Phobos and Deimos. The mission requires images with resolutions below 0.3 m for landing site selection. To satisfy this requirement, we set the performance requirements for TENGOO at iFoV < 6 μrad/pix, MTF at Nyquist frequency > 0.2, and SNR > 30. We equip OROCHI seven bandpass imagers and set its performance requirements at iFoV < 0.5 mrad/pix, MTF at Nyquist frequency > 0.2, and SNR > 100. In the preliminary design, TENGOO has a camera and interface component, and the optical system of TENGOO is catadioptric Cassegrain. TENGOO's design iFoV is 5.9 μrad/pix and its MTF at Nyquist frequency is 0.29. The temperature of the telescope will be maintained at $+20 \pm 5$ °C during observation to achieve MTF at Nyquist frequency > 0.2. OROCHI's camera and interface sub-assemblies combine into a single housing. The camera sub-assembly is composed of seven optics, seven bandpass filters, and seven CCD image sensors for multi-band imaging. Besides, OROCHI has a monochromatic camera for observation during the landing phase. The iFoVs are 0.44–0.46 mrad/pix, MTF at Nyquist frequency is above 0.3, and SNR is > 100 in nominal operation. We need longer exposure time when we obtain the image of the surface in the shadow of the spacecraft using the LED illumination because the surface brightness is 1/100 of the sunlit surface. We have to use 2×2 binning mode and the required exposure times to achieve SNR > ~100.

Abbreviations
ADC: Analog to digital conversion; AFE: Analog front-end electronics; CCD: Charge coupled device; CMDM: Circum-Martian dust monitor; FoV: Field of view; iFoV: Instantaneous field of view; FPGA: Field-programmable gate array; JAXA: Japan Aerospace Exploration Agency; LED: Light emitting diode; LIDAR: LIght detection and ranging; MEGANE: Mars-moon Exploration with GAmma rays and Neutrons; MIRS: MMX-InfRared Spectrometer; MMX: Martian Moon eXplorer; MSA: Mass spectrum analyzer; MTF: Modulation transfer function; ONC-T: Optical navigation camera telescope; OROCHI: Optical RadiOmeter composed of CHromatic Imagers; QSO: Quasi Satellite orbit; SERDES: SERializer DESerializer; SNR: Signal-to-noise ratio; SpW: SpaceWire; TENGOO: Telescopic Nadir Imager for GeOmOrphology.

Acknowledgements
This study is supported by the following grants: Japan Society for the Promotion of Science (JSPS) KAKENHI 17KK0097; 19H00727. We thank Ms. Shiho Kobayashi (Tohoku University), Dr. Isao Yoda (Laboratory for Advanced Nuclear Energy, TiTech), Dr. Kazuo Tanaka (Cyclotron and Radioisotope Center (CYRIC), Tohoku University), and JAXA MMX system team member for their support.

Authors' contributions
SK contributed to the design and development of the instrument and writing. MO, HK, CLK, YG, HM, SF, TA, KH, SM, NT, TT, KI, TO, TI, PH, RI contributed to the design of electronics, selection of detector, structural and thermal design. KE, RF, NO, KM, MM, KT, HS contributed to the optical design. All others provided feedback. All authors read and approved the final manuscript.

Funding
TENGOO and OROCHI instruments are financed by JAXA. This study is supported by the following grants: Japan Society for the Promotion of Science (JSPS) KAKENHI 17KK0097; 19H00727.

Availability of data and materials
Not applicable.

Declarations

Competing interests
The authors declare that they have no competing interest.

Author details
[1]Rikkyo University, Tokyo, Japan. [2]ISAS/JAXA, Tokyo, Japan. [3]Nihon University, Chiba, Japan. [4]AIST, Tokyo, Japan. [5]Meiji University, Tokyo, Japan. [6]The University of Tokyo, Tokyo, Japan. [7]Tohoku University, Tokyo, Japan. [8]PERC/Chitech, Chiba, Japan. [9]The Wakasa Wan Energy Research Center, Tsuruga, Japan. [10]National Central University, Taoyuan, Taiwan. [11]MEISEI, Tokyo, Japan. [12]NIKON, Tokyo, Japan.

Received: 20 January 2021 Accepted: 12 June 2021
Published online: 14 December 2021

References
Barruci MA et al (2021) MIRS an Imaging spectrometer for the MMX mission. Earth Planets Space https://doi.org/10.1186/s40623-021-01423-2
Fraeman AA et al (2014) Spectral absorptions on Phobos and Deimos in the visible/near infrared wavelengths and their compositional constraints. Icarus 229:196–205
Fujiya W et al (2021) Analytical protocols for Phobos regolith samples returned by the Martian Moons eXploration (MMX) mission. Earth Planets Space 73(1):1–24. https://doi.org/10.1186/s40623-021-01438-9
Kameda S et al (2017) Preflight calibration test results for optical navigation camera telescope (ONC-T) Onboard the Hayabusa2 Spacecraft. Space Sci Rev 208:17–31
Kruger H et al (2021) Modelling cometary meteoroid stream traverses of the Martian Moons eXploration (MMX) spacecraft en route to Phobos. Earth Planets Space https://doi.org/10.1186/s40623-021-01412-5
Kuramoto K et al (2021) Martian moons exploration MMX: sample return mission to Phobos elucidating formation processes of habitable planets. Earth Planets Space https://doi.org/10.1186/s40623-021-01545-7
Lawrence DJ et al (2019) Measuring the Elemental Composition of Phobos: The Mars-moon Exploration with GAmma rays and NEutrons (MEGANE) Investigation for the Martian Moons eXploration (MMX) Mission. Earth Space Sci 6:2605–2623
Michel P et al (2021) The MMX rover: performing in-situ surface investigations on Phobos. Earth Planets Space https://doi.org/10.1186/s40623-021-01464-7
Nakamura T, Ikeda H, Kouyama T, Nakagawa H, Kusano H, Senshu H, Kameda S, Matsumoto K, Gonzalez-Franquesa F, Ozaki N, Takeo Y (2019) Science Operation Plan of Phobos and Deimos From the MMX Spacecraft
Ogohara K et al (2021) The Mars system revealed by the Martian Moons eXploration mission. Earth Planets Space https://doi.org/10.1186/s40623-021-01417-0
Senshu H et al (2021) Light Detection and Ranging (LIDAR) laser altimeter for Martian Moons Exploration (MMX) spacecraft. Earth Planets Space https://doi.org/10.1186/s40623-021-01537-7
Thomas et al (2000) Phobos: Regolith and ejecta blocks investigated with Mars Orbiter Camera images. J Geophys Res 105:15091–15106
Usui et al (2020) The importance of phobos sample return for understanding the mars-moon system. Space Sci Rev 216:49
Yokota S et al (2021) In situ observations of ions and magnetic field around Phobos: The Mass Spectrum Analyzer (MSA) for the Martian Moons eXploration (MMX) mission. Earth Planets Space https://doi.org/10.1186/s40623-021-01452-x

Publisher's Note